

Free Volume and Oxygen Transport in Cold-Drawn Polyesters

R. Y. F. LIU, A. HILTNER, E. BAER

Department of Macromolecular Science, and Center for Applied Polymer Research, Case Western Reserve University, Cleveland, Ohio 44106-7202

Received 15 June 2003; revised 21 July 2003; accepted 19 August 2003

ABSTRACT: Poly(ethylene terephthalate) (PET), poly(ethylene terephthalate-co-4,4'-bibenzoate) (PETBB55), and poly(ethylene 2,6-naphthalate) (PEN) were cold-drawn to achieve uniform extension without crystallization or stress whitening, and oxygen transport properties were studied at temperatures from 10 to 40 °C. Correlation of oxygen solubility and polymer specific volume made it possible to consider the oriented polyester as a one-phase densified glass. Orientation was viewed as decreasing the amount of excess-hole free volume and bringing the nonequilibrium polymer glass closer to the equilibrium condition. Between 10 and 40 °C, the amount of excess-hole free volume in PET decreased as the polymer approached the glass transition temperature. In contrast, temperature changes in this range had little effect on the excess-hole free volume in PETBB55 and PEN, which were well below their glass transition temperature. Gas diffusion was viewed as discrete jumps of the oxygen molecule between holes of excess-free volume. The jump length was extracted from the activation energy for diffusion according to a channel-formation model. The result agreed well with the hole spacing estimated from a simple lattice model using the hole density reported in the literature. Extending the lattice model to estimate the mean excess-free volume hole radius from the fractional free volume resulted in good correlation with the hole radius obtained from positron annihilation lifetime spectroscopy. © 2003 Wiley Periodicals, Inc. *J Polym Sci Part B: Polym Phys* 42: 493–504, 2004

Keywords: poly(ethylene terephthalate); poly(ethylene 2,6-naphthalate); poly(ethylene terephthalate-co-benzoate); orientation; free volume; oxygen transport; diffusion; permeability; solubility

INTRODUCTION

Poly(ethylene terephthalate) (PET) is widely used in packaging applications that require high gas barrier characteristics. Crystallinity and structural asymmetry imparted by orientation have profound effects on gas transport. Indeed, optimizing these features is essential for achieving the highest barrier. Efforts to understand the structural basis of gas permeability were pio-

neered by Ward and coworkers, who systematically altered the solid-state structure of PET and other polymers by orientation and crystallization.^{1,2} These studies revealed the shortcomings of simple two-phase models that considered only an impermeable crystalline phase and a permeable amorphous phase with unique barrier characteristics. It was apparent that processing history impacted the amorphous phase in ways that affected gas permeation. The studies of Ward and coworkers also suggested that gas transport could be a powerful probe of the solid-state structure if used in conjunction with other characterization tools.³

Correspondence to: A. Hiltner (E-mail: pah6@po.cwru.edu)

Journal of Polymer Science: Part B: Polymer Physics, Vol. 42, 493–504 (2004)
© 2003 Wiley Periodicals, Inc.

These findings motivated us to probe further for structural models of gas transport in PET and other aromatic polyesters. In these efforts, the molecular scale concepts embodied in the free-volume model of gas transport in glassy polymers were particularly useful.⁴ Conceptually, permeation of small gas molecules through a glassy polymer is viewed as proceeding by jump motion whereby a permeant molecule spends most of the time in free-volume cavities and occasionally jumps to a neighboring cavity. The jump motion proceeds by formation of a channel between two neighboring holes. Thus gas permeation depends on the number and size of cavities in the polymer matrix (static free volume) and the frequency of channel formation (dynamic free volume). Static free volume is essentially independent of thermally accessible motions of the polymer chains and relates to gas solubility S . Dynamic free volume derives from accessible conformational changes and segmental motions of the polymer chain and relates to gas diffusivity D .

The free volume approach to gas transport provides molecular scale insight into the glassy state. For oxygen at 1 atm pressure, the contribution of matrix dissolution is negligible in aromatic polyesters, and gas sorption is viewed as the process of filling holes of free volume. Gas solubility should be proportional to the excess-hole free volume trapped within the glassy polymer upon cooling below T_g . Indeed, a linear relationship between oxygen solubility S at 25 °C and 1 atm and amorphous phase specific volume ν_a has been observed for many aromatic polyesters including glassy copolymers of PET,^{5,6} cold-drawn PEN, PET, and a PET copolymer,⁷ and for the amorphous phase of crystallized PET,⁸⁻¹⁰ and PEN.¹¹ Extrapolation gives ν_o , the specific volume at zero solubility, and the quantity $(\nu_a - \nu_o)$ identifies the excess-hole free volume available to oxygen. Orientation of the glassy state decreases excess-hole free volume, whereas crystallization often has the effect of "dedensifying" the amorphous phase and thereby increasing the excess-hole free volume as measured by the change in S of the amorphous phase. It is apparent from examination of oxygen transport characteristics of many aromatic polyesters that dynamic free volume, which relates to D , does not correlate with excess-hole free volume from S .^{5,6} Because both S and D determine permeability, the large scatter encountered in efforts to predict permeability of common gases in a wide array of glassy polymers by empirical application

of the free-volume concept inevitably encounter large scatter.^{12,13}

In a fairly narrow window of stretching conditions near the glass transition temperature it is possible to achieve uniform orientation of polyesters without crystallization or stress whitening.^{7,14} Oxygen solubility of cold-drawn polyesters follows a linear dependence on specific volume. This makes it possible to view the oriented polymer as a one-phase glass and to consider the orientation process as decreasing the amount of excess-hole free volume. We now extend our investigation of oriented, glassy polyesters to consider the effect of temperature on oxygen transport and address the role of diffusivity in the transport process. Additional measurements of free volume hole size by positron annihilation lifetime spectroscopy lead to a physical picture of gas sorption and diffusion in the glassy state based on a simple lattice-hole model.

MATERIALS AND METHODS

Pellets of poly(ethylene terephthalate) (PET), a copolymer based on PET, poly(ethylene terephthalate-co-4,4' bibenzoate), in which 55 mol % of the terephthalate was replaced with bibenzoate (PETBB55), poly(ethylene 2,6-naphthalate) (PEN), and poly(ethylene isophthalate) (PEI) were supplied by KoSa (Spartanburg, SC). The polyesters were polymerized according to the methodology described previously.⁵ The intrinsic viscosity was measured at 25 °C in 1% (w/w) dichloroacetic acid solution. The intrinsic viscosities were 0.84, 0.83, 0.64, and 0.75 dL g⁻¹ for PET, PETBB55, PEN, and PEI, respectively. The glass transition temperatures measured by DSC were 79, 104, 124, and 68 °C, respectively.^{5,7}

Compression-molded amorphous films were cold-drawn under constrained uniaxial conditions, that is, temperatures at which the polymers would not crystallize, to a target draw ratio as described previously.⁷ The draw temperatures were 70, 80, and 144 °C for PET, PETBB55, and PEN, respectively. The draw rate was 20 mm min⁻¹ for PET and PEN, and 5 mm min⁻¹ for PETBB55. Four draw ratios were obtained for each polymer. The initial film thickness was chosen to achieve a final film thickness between 150 and 200 μm . The highest draw ratio λ was 3.8 for PET, 6.0 for PETBB55, and 4.8 for PEN. The cold-drawn films were determined to be noncrystalline by wide-angle X-ray diffraction (WAXD)

instead of differential scanning calorimetry (DSC).^{15,16}

A density gradient column was constructed from a solution of calcium nitrate and water in accordance with ASTM D Standard 1505 Method B. The column was calibrated with glass floats of known density and thermal expansivity. Small pieces of quenched and oriented films (ca. 25 mm²) were placed in the column. To measure density in the temperature range from 5 to 50 °C, a circulating water bath was connected to the jacket of the density column. Temperature measured in the density column was controlled to ± 0.5 °C. The column was held at temperature for 2 h before the density measurement was made. The linearity of the calibration curve was characterized by $r^2 > 0.997$. Averages of four measurements at each temperature were reported. The accuracy was ± 0.0009 g cm⁻³.

Positron annihilation lifetime spectroscopy (PALS) was performed using the fast-fast coincident method with a time resolution of 230 ps,¹⁷ at a count rate of approximately 1 million counts per hour. The positron lifetime τ was determined by PATFIT software. The spectra were fitted to three exponentially decaying lifetime components. The longest lived component with lifetime τ_3 corresponded to the pickoff annihilation of *ortho*-positronium (*o*-Ps) in the free-volume holes of the polymer matrix, from which the mean free volume hole radius r was calculated.¹⁷ The uncertainty in r based on 10 spectra was ± 0.02 Å.

Oxygen flux $J(t)$ at 0% relative humidity and 1 atm pressure was measured with a MOCON OX-TRAN 2/20. The instrument was calibrated with NIST-certified Mylar[®] film of known oxygen transport characteristics. The temperature in the diffusion cell was varied from 10 to 40 °C with an accuracy of ± 0.1 °C. Specimens were carefully conditioned as described previously.⁸ To obtain the diffusivity D and to accurately determine the permeability P , the data were fit to the solution of Fick's second law with appropriate boundary conditions⁸

$$J(t) = \frac{Pp}{l} \left[1 + 2 \sum_{n=1}^{\infty} (-1)^n \exp\left(-\frac{D\pi^2 n^2 t}{l^2}\right) \right] \quad (1)$$

The thickness l of each specimen was determined from the measured density after the barrier measurement was completed.⁸ Most of the specimens were tested within 30 days of orienta-

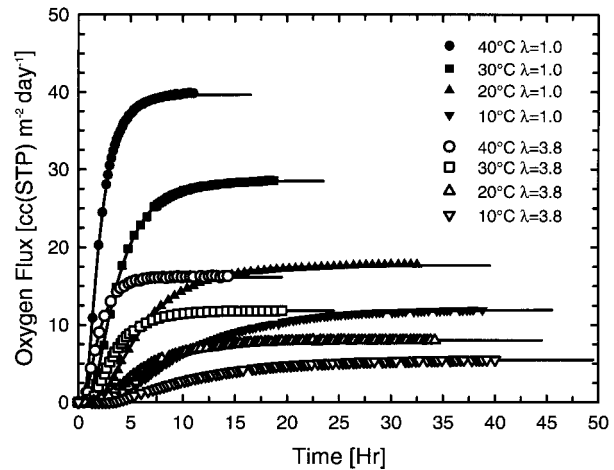


Figure 1. Experimental oxygen flux data and fit to eq. (1) (solid lines) for quenched and cold-drawn PET films at various temperatures.

tion. Films were determined to be fully relaxed when retesting at 25 °C after the films were tested at elevated temperatures produced the same oxygen flux as the initial test at 25 °C.

RESULTS AND DISCUSSION

Excess Free Volume from Oxygen Sorption

The effect of orientation on PET oxygen flux at various temperatures is shown in Figure 1. Comparison of flux curves for $\lambda = 1$ and $\lambda = 3.8$ indicated that cold-drawing affected both the nonsteady-state and steady-state parts of the oxygen-flux curve. The nonsteady-state region broadened (slower diffusion) and the steady-state flux decreased (lower permeability). Comparison of flux curves for four temperatures indicated that decreasing temperature also broadened the nonsteady state region and decreased the steady-state flux. Results for PEN and PETBB55 showed the same trends. The fitting curves to eq. (1) from which P and D were obtained are included with the experimental data points. Solubility S was calculated from the relationship $S = PD^{-1}$. The fit of the flux curves to eq. (1) was equally good for all the experiments. The results are compiled in Tables 1, 2, and 3. The results for P , D , and S of PET at 25 °C and 1 atm matched literature values obtained with a pressure cell and the time-lag method of analysis.^{18,19}

Specific volume of PET in the temperature range 5–50 °C is shown in Figure 2. The linear

Table 1. Effect of Orientation and Temperature on the Physical Properties of PET

Material	T (°C)	ρ (g cm ⁻³)	P	$D \times 10^{13}$	S	ν_f (cm ³ g ⁻¹)	FFV
PET $\lambda = 1.0$	10	1.3420	0.245	2.3	0.123	0.031	0.041
	15	1.3400	0.304	3.0	0.117	0.030	0.040
	20	1.3379	0.384	4.0	0.111	0.029	0.039
	25	1.3359	0.463	5.2	0.103	0.029	0.038
	30	1.3339	0.575	6.9	0.096	0.027	0.037
	35	1.3319	0.678	8.8	0.089	0.027	0.036
	40	1.3299	0.787	11.3	0.081	0.025	0.034
PET $\lambda = 2.1$	10	1.3441	0.220	2.1	0.121	0.030	0.040
	15	1.3422	0.264	2.7	0.113	0.028	0.038
	20	1.3403	0.334	3.7	0.104	0.028	0.037
	25	1.3385	0.405	4.8	0.098	0.027	0.036
	30	1.3366	0.504	6.4	0.091	0.026	0.035
	35	1.3347	0.595	8.4	0.082	0.025	0.033
	40	1.3329	0.718	10.8	0.077	0.024	0.032
PET $\lambda = 3.1$	10	1.3568	0.145	1.8	0.093	0.022	0.030
	15	1.3551	0.171	2.4	0.082	0.021	0.028
	20	1.3533	0.213	3.2	0.077	0.020	0.027
	25	1.3516	0.267	4.3	0.072	0.020	0.027
	30	1.3498	0.315	5.7	0.064	0.018	0.025
	35	1.3481	0.364	7.4	0.057	0.017	0.023
	40	1.3464	0.422	9.6	0.051	0.016	0.021
PET $\lambda = 3.8$	10	1.3625	0.107	1.6	0.077	0.020	0.027
	15	1.3607	0.129	2.1	0.071	0.018	0.025
	20	1.3589	0.162	2.8	0.067	0.018	0.024
	25	1.3571	0.195	3.7	0.061	0.017	0.023
	30	1.3553	0.238	5.0	0.055	0.016	0.021
	35	1.3536	0.279	6.6	0.049	0.015	0.020
	40	1.3518	0.327	8.8	0.043	0.013	0.018

P—Permeability (cc[STP] cm m⁻² atm⁻¹ day⁻¹).

D—Diffusivity (m² s⁻¹).

S—Solubility (cc[STP] cm⁻³ atm⁻¹).

relationship was described by the expression, $\nu = \nu' + T e_g$, which gave the extrapolated specific volume at 0 K as ν' and thermal expansivity as e_g . The results are summarized in Table 4. Quenched PET, PETBB55, and PEN had approximately the same specific thermal expansivity of 2.2×10^{-4} cm³ g⁻¹ K⁻¹, which was identical to the value reported in the literature for PET.²⁰ Orientation slightly decreased the thermal expansivity.

The relationship between S and ν ($\nu = \rho^{-1}$) for cold-drawn polymers is plotted in Figure 3. The decrease in S with increasing draw ratio followed the densification line observed previously.⁷ The linear relationship is expressed as

$$S = \beta(\nu - \nu_o) = \beta\nu_f \quad (2)$$

where ν_o is the specific volume at zero solubility. Extrapolations gave ν_o for each temperature. A

linear relationship between S and ν at 25 °C and 1 atm was observed previously for glassy copolymers of PET,^{5,6} for cold-drawn PET, PEN, and PETBB55,⁷ and for the amorphous phase of crystallized PET⁸⁻¹⁰ and PEN.¹¹ The linear relationship appears to be a common characteristic of polyesters of ethylene glycol and aromatic diacids. According to free-volume concepts that view sorption as the process of filling holes of static free volume, the quantity $\nu_f = \nu - \nu_o$ identifies the excess-hole free volume available to oxygen,^{5,21} which can also be expressed as fractional free volume $FFV = \nu_f/\nu$. The listed ν_f and FFV values in Tables 1, 2, and 3 are calculated from $\nu_f = S/\beta$. It follows that orientation of the glassy state decreases the excess-hole free volume. The slope β reflects the density of sorbed oxygen.

Both lower free volume and lower sorbed oxygen density could have contributed to the overall

Table 2. Effect of Orientation and Temperature on the Physical Properties of PETBB55

Material	T (°C)	ρ (g cm ⁻³)	P	$D \times 10^{13}$	S	ν_f (cm ³ g ⁻¹)	FFV
PETBB55 $\lambda = 1.0$	10	1.3134	0.360	3.0	0.139	0.032	0.042
	18	1.3105	0.461	4.3	0.124	0.031	0.041
	25	1.3080	0.650	6.6	0.114	0.030	0.039
	33	1.3052	1.018	11.3	0.104	0.031	0.040
	40	1.3027	1.346	16.4	0.095	0.031	0.040
PETBB55 $\lambda = 3.0$	10	1.3302	0.156	1.8	0.100	0.023	0.030
	18	1.3274	0.242	3.1	0.090	0.023	0.030
	25	1.3249	0.294	4.2	0.081	0.021	0.028
	33	1.3222	0.467	7.5	0.072	0.021	0.028
	40	1.3197	0.628	11.4	0.064	0.021	0.027
PETBB55 $\lambda = 4.0$	10	1.3404	0.076	1.2	0.073	0.017	0.022
	18	1.3377	0.097	1.8	0.062	0.015	0.020
	25	1.3354	0.147	3.1	0.055	0.014	0.019
	33	1.3328	0.246	5.7	0.050	0.015	0.020
	40	1.3305	0.335	8.6	0.045	0.015	0.019
PETBB55 $\lambda = 6.0$	10	1.3464	0.039	0.76	0.059	0.013	0.018
	18	1.3438	0.053	1.3	0.047	0.012	0.016
	25	1.3416	0.085	2.3	0.043	0.011	0.015
	33	1.3390	0.136	4.0	0.039	0.011	0.015
	40	1.3367	0.186	6.1	0.035	0.011	0.015

P—Permeability (cc[STP] cm m⁻² atm⁻¹ day⁻¹).

D—Diffusivity (m² s⁻¹).

S—Solubility (cc[STP] cm⁻³ atm⁻¹).

decrease in oxygen solubility as the temperature rose. The plots in Figure 3 separated these two factors and revealed how temperature affected static free volume and sorbed gas density. In all cases, ν_o increased and β decreased as the temperature rose. For PET, which was closest to T_g , the increase in ν_o was most noticeable. Increasing temperature reduced the FFV of isotropic quenched PET from 0.041 to 0.034. The change in S primarily reflected the decrease in FFV as the temperature approached T_g .

Although the same trends in the S versus ν relationship were observed for PETBB55 and PEN, the increase in ν_o was weaker. For these polymers, which were well below T_g , FFV of the isotropic quenched glass remained almost constant through the temperature range studied (Tables 2 and 3). For PETBB55, FFV decreased only from 0.042 to 0.040 for the isotropic quenched glass; for PEN the decrease was from 0.047 to 0.043. The decrease in S as the temperature rose was primarily due to lower density of sorbed gas.

The slope β reflects the density of sorbed oxygen ρ_{O_2} in the excess-hole free volume. The relationship between β and ρ_{O_2} is given by:⁵

$$\rho_{O_2} = \frac{\nu\beta p M_w}{22,400} \quad (3)$$

where ν is the specific volume of the glassy polymer, $p = 1$ atm is the oxygen pressure, and $M_w = 32$ g mol⁻¹ is the molecular weight of oxygen. In the temperature range from 10 to 40 °C, the sorbed oxygen density in PET decreased from 4.4×10^{-3} to 3.4×10^{-3} g per cm³ of excess-hole free volume (Table 5). Assuming ideal gas behavior, the corresponding oxygen pressure decreased from 3.4 to 2.6 atm. Essentially the same values were observed for PETBB55 and PEN. Although the effect of temperature on FFV differed somewhat between PET and the other polymers, the state of sorbed oxygen, as indicated by gas density, did not depend on polymer characteristics such as T_g .

Because of the long time scale required for glassy polymers to relax fully, gas transport typically occurs under nonequilibrium conditions wherein the polymer possesses more free volume than it would at equilibrium. According to the concepts of Vrentas and Duda,²² the volume of the nonequilibrium glassy polymer is larger than the extrapolated equilibrium volume by the excess free volume. Previous studies of glassy polyesters^{5,7} demonstrate that the free volume accessible to oxygen molecules corresponds to the excess-hole free volume as described in the Vrentas and Duda model. Thus, the extrapolated zero-solubil-

Table 3. Effect of Orientation and Temperature on Physical Properties of PEN

Material	T (°C)	ρ (g cm ⁻³)	P	$D \times 10^{13}$	S	ν_f (cm ³ g ⁻¹)	FFV
PEN $\lambda = 1.0$	10	1.3330	0.080	0.61	0.152	0.035	0.047
	18	1.3299	0.129	1.1	0.136	0.035	0.046
	25	1.3272	0.167	1.6	0.121	0.037	0.049
	29	1.3256	0.181	1.9	0.110	0.035	0.047
	33	1.3241	0.220	2.6	0.098	0.034	0.045
	36	1.3230	0.241	3.0	0.093	0.033	0.044
	39	1.3218	0.274	3.6	0.088	0.033	0.043
PEN $\lambda = 2.0$	10	1.3347	0.070	0.53	0.153	0.035	0.047
	18	1.3318	0.115	1.0	0.133	0.034	0.045
	25	1.3293	0.154	1.5	0.119	0.035	0.047
	29	1.3279	0.181	1.9	0.110	0.035	0.047
	33	1.3265	0.216	2.5	0.100	0.034	0.045
	36	1.3254	0.243	3.0	0.094	0.034	0.044
	39	1.3244	0.276	3.7	0.086	0.032	0.042
PEN $\lambda = 3.5$	10	1.3520	0.031	0.30	0.120	0.028	0.038
	18	1.3491	0.044	0.51	0.100	0.026	0.035
	25	1.3465	0.060	0.82	0.085	0.026	0.035
	29	1.3451	0.071	1.1	0.075	0.025	0.033
	33	1.3436	0.086	1.4	0.071	0.024	0.032
	36	1.3425	0.098	1.7	0.067	0.024	0.032
	39	1.3414	0.112	2.1	0.062	0.023	0.031
PEN $\lambda = 4.8$	10	1.3565	0.014	0.17	0.095	0.023	0.031
	18	1.3538	0.023	0.31	0.086	0.022	0.030
	25	1.3515	0.032	0.50	0.074	0.023	0.031
	29	1.3502	0.039	0.67	0.067	0.022	0.030
	33	1.3488	0.046	0.85	0.063	0.021	0.029
	36	1.3479	0.053	1.1	0.056	0.021	0.028
	39	1.3469	0.058	1.3	0.052	0.019	0.026

P—Permeability (cc[STP] cm m⁻² atm⁻¹ day⁻¹).

D—Diffusivity (m² s⁻¹).

S—Solubility (cc[STP] cm⁻³ atm⁻¹).

ity specific volume ν_o represents a point on the equilibrium curve.

Orientation by cold-drawing is viewed as decreasing the excess-hole free volume and bringing

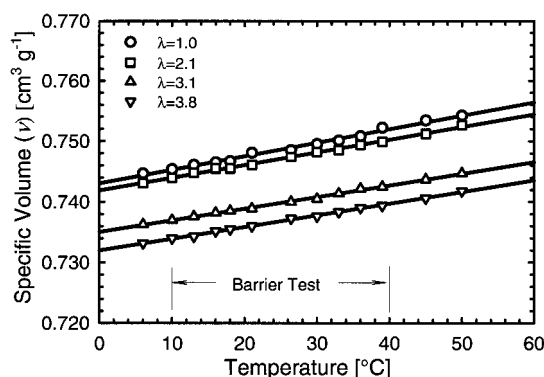


Figure 2. Thermal expansion curves of quenched and cold-drawn PET.

the nonequilibrium polymer glass closer to the equilibrium line. Orientation to the maximum draw ratio decreased the excess-hole free volume ν_f by a fraction of 0.41, 0.63, and 0.38 for PET, PETBB55, and PEN, respectively, at 25 °C. The closest approach to ν_o was obtained with PETBB55. The relative ease with which free volume could be removed from PETBB55 by orientation reflected the frustrated liquid crystalline nature of this polymer.^{7,23,24}

The orientation effect is incorporated into the thermal expansion (V - T curve) of polyesters in Figure 4. As described previously,^{5,7} the temperature is normalized to the glass transition temperature T_g , whereas the specific volume is normalized to that of PET, assuming the same thermal expansivity for glass, 2.2×10^{-4} cm³ g⁻¹, and for liquid, 7.0×10^{-4} cm³ g⁻¹.²⁰ The core expansion curve $\eta_o(T)$ is taken from a previous publica-

Table 4. Effect of Orientation on Thermal Expansion of Polyesters

Material	λ	ν' ($\text{cm}^3 \text{g}^{-1}$)	$(10^{-4} \text{ cm}^3 \text{g}^{-1} \text{K}^{-1})$
PET ($T_g = 79 \text{ }^\circ\text{C}$)	1.0	0.6812	2.26
	2.1	0.6848	2.09
	3.1	0.6800	1.91
	3.8	0.6821	1.94
PETBB55 ($T_g = 104 \text{ }^\circ\text{C}$)	1.0	0.7025	2.08
	3.0	0.6957	1.98
	4.0	0.6937	1.85
	6.0	0.6918	1.80
PEN ($T_g = 124 \text{ }^\circ\text{C}$)	1.0	0.6882	2.19
	2.0	0.6921	2.02
	3.5	0.6819	2.04
	4.8	0.6860	1.81

tion,⁵ and is based on the specific excess-hole free volume, calculated from the oxygen solubility, of many glassy polyesters. The excess-hole free volume removed by orientation (the difference between ν at $\lambda = 1$ and ν at $\lambda > 1$) is calculated according to eq. (2) with slope β at each temperature and subtracted from the $\nu(T)$ line for isotropic, unoriented PET at the appropriate value of $T - T_g$. Additional points for oriented PET, PETBB55, and PEN for various $T - T_g$ show how the specific volume approaches the equilibrium $\nu_o(T)$ curve with increasing orientation. Taken together, experimental values of ν_o from the three polyesters cover the temperature range from $T_g - 39$ to $T_g - 114$ K. Fairly good agreement was obtained between the $\nu_o(T)$ from this study (data points) and previous results (solid line).⁵ The consistency in ν_f among different polyesters reflects the common characteristics of excess-hole free volume in the glassy state. At low $T - T_g$ the fractional free-volume FFV approaches a constant value of 0.05, which is in between the estimated FFV values based on the WLF equation (0.025),²⁵ and a simple extrapolation of the liquid expansion curve (0.11).²⁶ Furthermore, values of FFV are in line with estimations for glassy polymers based on molecular simulations,⁴ and group contributions.¹²

Oxygen Diffusion by Channel Formation

Gas diffusion through polymers in the glassy state is generally viewed as taking place by discrete jumps. In the free-volume model, the jump motion proceeds by formation of a channel be-

tween two neighboring holes of static-free volume. The frequency of channel formation defines the dynamic free volume and derives from accessible conformational changes and segmental motions of the polymer chain. The exponential temperature dependence of D is characteristic of an activated process that can be described by the Arrhenius equation²⁷

$$D = D_o \exp\left(-\frac{E_D}{RT}\right) \quad (4)$$

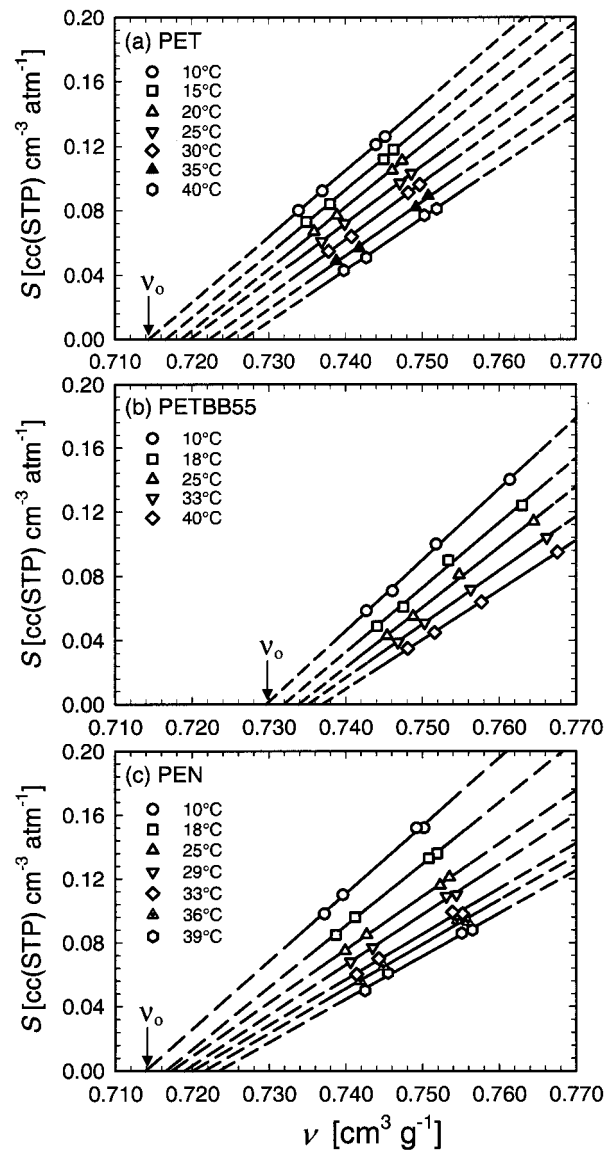


Figure 3. Relationship between oxygen solubility and specific volume ($\nu = \rho^{-1}$): (a) PET; (b) PETBB55; and (c) PEN.

Table 5. Effect of Temperature on Sorbed Oxygen Properties

Material	T (°C)	β (cc[STP] g cm ⁻⁶ atm ⁻¹)	ν_o (cm ³ g ⁻¹)	$(10^{-3} \rho_{O_2})$ (g cm ⁻³)	P_{O_2} (atm)
PET	10	4.1	0.714	4.4	3.4
	15	4.0	0.716	4.3	3.3
	20	3.8	0.718	4.1	3.1
	25	3.6	0.720	3.8	3.0
	30	3.5	0.722	3.7	2.9
	35	3.3	0.724	3.5	2.7
PETBB55	40	3.2	0.727	3.4	2.6
	10	4.4	0.730	4.8	3.7
	18	4.0	0.732	4.4	3.4
	25	3.8	0.734	4.2	3.2
	33	3.4	0.735	3.7	2.9
PEN	40	3.1	0.737	3.4	2.6
	10	4.3	0.714	4.6	3.6
	18	3.9	0.717	4.2	3.3
	25	3.3	0.718	3.6	2.8
	29	3.1	0.719	3.3	2.6
	33	2.9	0.720	3.1	2.4
	36	2.8	0.722	3.0	2.3
	39	2.7	0.724	2.9	2.3

where E_D is the activation energy. The temperature dependence of permeability is similarly described by

$$P = P_o \exp\left(-\frac{E_P}{RT}\right) \quad (5)$$

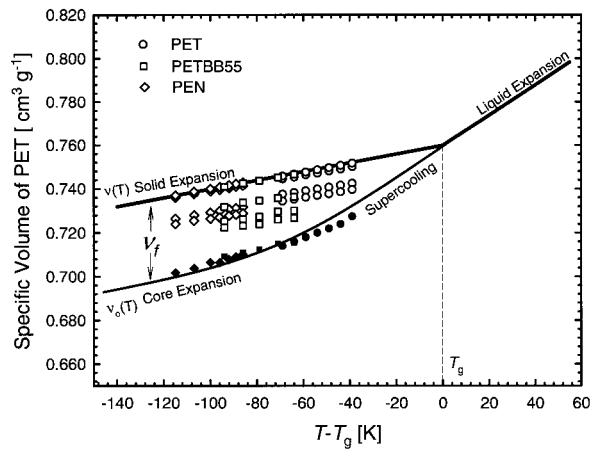


Figure 4. Specific volume versus temperature relationship constructed for amorphous PET with oxygen solubility as a measure of excess-hole free volume and including the effect of temperature and orientation. The filled symbols represent points on the equilibrium curve.

where E_P is the activation energy for permeation. The temperature dependence of P and D , plotted in Figure 5 for PETBB55, shows good correspondence with eq. (4) and eq. (5) in the temperature range from 10 to 40 °C. Orientation tends to increase E_D and E_P , except for E_P of PET. The energetic parameters are compiled in Table 6. Values for PET and PEN match previous reports.^{5,11}

A mechanistic interpretation of E_D was first proposed by Meares for diffusion of simple gases in rubbery polymers and extended to the glassy state where the activated diffusion mechanism is well established.^{13,28-30} In this model, the polymer is regarded as randomly oriented regions of roughly parallel polymer segments. By analogy with the quasi-crystalline picture of a liquid, creation of a channel involves complete separation beyond the limit of van der Waals interaction for the diffusing gas molecule. The energy required to create a channel of cross-sectional area $\pi d^2/4$ and length α equals the energy required to break the physical bonds between the polymer segments

$$E_D = \frac{1}{4} \pi d^2 \alpha CED N_A \quad (6)$$

where, E_D is the activation energy for diffusion in J mol⁻¹, d is the collision diameter of the gas

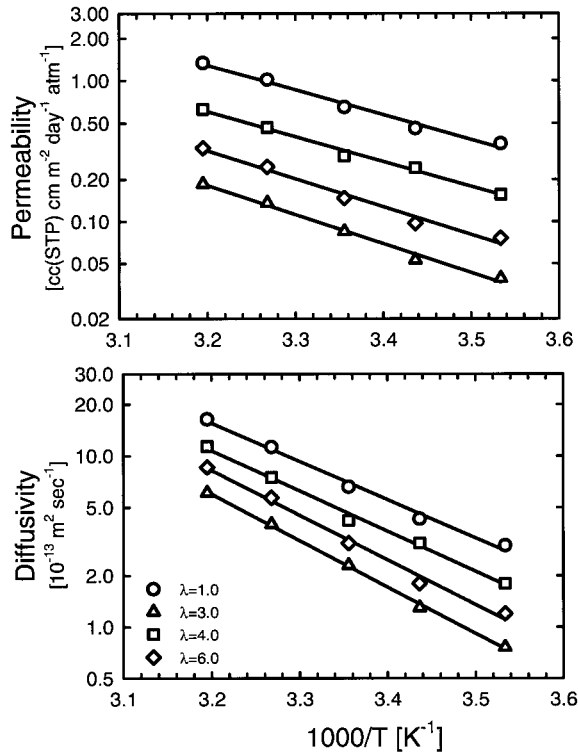


Figure 5. Temperature dependence of permeability and diffusivity for quenched and cold-drawn PETBB55 films.

penetrant in m, α is the jump length in m, CED is the cohesive energy density of the polymer in J m^{-3} , and N_A is Avogadro's number. Values of the calculated jump length α from eq. (6), where the collision diameter of oxygen is taken as 3.47 \AA , and CED is calculated from group contributions,²⁰ are summarized in Table 7. According to

the concept expressed by eq. (6), similarity in activation energy for diffusion translates to similar diffusional jump lengths of approximately 14 \AA for all the polyesters studied. These values correlate well with the results of molecular simulations.³¹

A simple calculation can test whether the results are reasonable. For simplicity, excess free-volume holes are assumed to be arranged on a cubic lattice. This concept is similar to the lattice models used to describe both rubbery and glassy states.^{32,33} Diffusion is viewed as the process of a gas molecule jumping from one lattice site to a neighboring lattice site. Various PALS studies, considering either an average hole size,^{34–36} or a distribution of hole sizes,³⁷ yield a free volume hole density N_o of about $4.0 \times 10^{20} \text{ cm}^{-3}$ for a wide range of polymers. The jump length from the lattice model α_m is then defined by the hole density as

$$\alpha_m = \frac{1}{\sqrt[3]{N_o}} \quad (7)$$

For N_o of $4.0 \times 10^{20} \text{ m}^{-3}$, α_m is 13.6 \AA in excellent agreement with the estimate of jump length α from E_D . The corresponding radius of uniform spherical holes r_m follows from the fractional free volume according to

$$r_m = \alpha_m \sqrt[3]{\frac{3FFV}{4\pi}} \quad (8)$$

where FFV is obtained from oxygen solubility (Tables 1–3). The calculated hole radius r_m decreases

Table 6. Effect of Orientation on Activation Energies for Oxygen Permeation and Diffusion

Material	λ	$\ln P_o$ (P_o in cc[STP] $\text{cm m}^{-2} \text{ day}^{-1} \text{ atm}^{-1}$)	E_P (kJ mol^{-1})	$\ln D_o$ (D_o in $\text{m}^2 \text{ sec}^{-1}$)	E_D (kJ mol^{-1})
PET	1.0	10.9	29.0	-12.4	39.7
	2.1	11.0	29.4	-11.9	40.6
	3.1	9.5	26.9	-11.8	41.2
	3.8	9.6	27.8	-11.6	42.7
PETBB55	1.0	13.2	33.6	-10.7	42.8
	3.0	12.5	33.8	-10.3	44.8
	4.0	13.6	38.2	-8.6	49.7
	6.0	13.6	39.9	-8.1	52.4
PEN	1.0	10.2	29.8	-11.7	44.0
	2.0	11.8	33.9	-10.1	48.1
	3.5	10.3	32.6	-10.2	49.0
	4.8	11.1	36.0	-9.8	51.0

Table 7. Lattice Parameters of Polyesters at 25 °C

Material	ρ (g cm ⁻³)	T_g (°C)	S (cc[STP] cm ⁻³ atm ⁻¹)	FFV	E_D (KJ mol ⁻¹)	CED (10 ⁸ J m ⁻³)	α from eq. (6) (Å)	r from PALS (Å)	r_m from eq. (8) (Å)
PEN	1.3272	124	0.121	0.049	39.7	5.3	14.5	2.59	3.1
PETBB55	1.3080	104	0.114	0.039	42.8	5.3	14.2	2.58	2.9
PET	1.3359	79	0.103	0.038	44.0	5.4	12.9	2.56	2.8
PEI	1.3509 ^a	68 ^a	0.072 ^a	0.027	43.0 ^a	5.5	13.7	2.41	2.5

^a ref. 5.

from 3.1 Å for PEN with the highest T_g to 2.5 Å for PEI with the lowest T_g . Values of the mean free volume hole radius r obtained independently by PALS were 2.59, 2.58, 2.56, and 2.41 Å for PEN, PETBB55, PET, and PEI, respectively (Table 7). The larger hole size obtained with oxygen is consistent with the larger radius of the oxygen molecule compared to the PALS probe particle radius.³⁸ The consistency among independent estimates of hole size and jump length supports the simple physical model that views gas diffusion as the random hopping of an oxygen molecule from one excess free volume hole to another. It should be emphasized, however, that this model applies under conditions where only low energy sorption sites participate in the transport process.

Low diffusivity of PEN ($D = 1.6 \times 10^{-13}$ m² s⁻¹, Table 3) compared to PET ($D = 5.2 \times 10^{-13}$ m² s⁻¹, Table 1) and PETBB55 ($D = 6.6 \times 10^{-13}$ m² s⁻¹, Table 2) at 25 °C cannot be ascribed to a difference in jump length. Indeed, from eq. (6), similarity in E_D means that α does not differ much among the four polyesters. The diffusivity D depends on jump length and also on the effective jump frequency ω as²⁷

$$D = \frac{1}{6} \omega \alpha^2 \quad (9)$$

For PET at 25 °C with D of 5.2×10^{-13} m² s⁻¹ (Table 1) and an average jump length of 12.9 Å, the calculated jump frequency ω is 1.9×10^6 s⁻¹, which means that one oxygen molecule makes one jump every 5.3×10^5 ps. If one takes the Debye frequency, kT/h or 6×10^{12} s⁻¹, as the oscillation frequency of the gas molecule, only one out of every 10^7 oscillations produces a successful jump from one hole to another. The time scale of the actual jump is on the order of several picoseconds from molecular simulations.³⁰ If the time spent in

jumping is compared with the time spent in the hole, over 99% of the time is spent in the hole. This conforms to the understanding that gas molecules sorbed in the polymer glass reside mostly in the holes rather than moving in the matrix.⁴

Recognizing that the diffusion mechanism is conserved, it follows that the jump frequency is much lower in PEN. From eq. (9), ω decreases from 1.9×10^6 and 2.0×10^6 s⁻¹ for PET and PETBB55, respectively, to 0.5×10^6 s⁻¹ for both PEI and PEN. Previous studies suggested that dynamic free volume of aromatic polyesters derives from segmental motions associated with the subambient γ -relaxation,⁵ and specifically with the intensity of the relaxation component attributed to *gauche* chain conformations.⁶ The *gauche* fraction from infrared spectroscopy is 0.75 for PEI,³⁹ and 0.79 for PEN;⁷ both are significantly lower than 0.91 and 0.93 for PET and PETBB55, respectively.⁷ Very likely, lower *gauche* fraction contributes to lower jump frequency and lower diffusivity of PEI and PEN.

It is now interesting to consider what fraction of the holes contains an oxygen molecule at any given instant. The density of sorbed oxygen in PET is 3.8×10^{-3} g per cm³ excess-hole free volume at 25 °C and 1 atm (Table 5). This is significantly smaller than the density of one gas molecule per hole, which would be 0.56 g per cm³ free volume estimated from a hole density of 4.0×10^{20} cm⁻³. This suggests that most of the holes are empty. The fraction of filled holes is estimated to be less than 1%. Statistically, less than 1 out of every 100 holes contains a gas molecule, and the probability that a hole contains two oxygen molecules is negligible. Nevertheless, if each permeant molecule jumps 1.8×10^6 times per second, all the holes will be probed many times over in 1 s.

Although the number of gas molecules sorbed in the glassy state is considerably smaller than

the number of accessible free volume holes, the sorbed gas is seen as occupying all the free volume through high jump frequency. The free volume holes are interconnected by diffusion channels, which are instantly opened and closed by subambient segmental relaxation as suggested previously.⁵ The fast jump rate justifies the concept of sorbed gas density because the gas molecules share all the free volume holes.

CONCLUSIONS

This study probes the temperature-dependence of oxygen transport in some oriented aromatic polyesters. At all temperatures, oxygen solubility of cold-drawn polyesters follows a linear dependence on specific volume. This is consistent with the view that orientation decreases the amount of excess-hole free volume. As the temperature increases toward T_g , both decreasing free volume and decreasing sorbed gas density can contribute to lower gas solubility. Although oxygen diffusivity at any temperature depends strongly on orientation and chemical structure of the polyester, neither variable has a strong effect on the activation energy for diffusion. This suggests that the fundamental diffusion mechanism does not change.

At 1 atm pressure, it appears that oxygen probes only the excess-hole free volume, and it is possible to consider a simple lattice model to describe oxygen transport. Oxygen molecules are viewed as residing in holes of excess-free volume and periodically jumping through a dynamic channel from one hole to another hole. Fractional free volume (the static free-volume component) is determined from the correlation between oxygen solubility and specific volume of the cold-drawn polyester. The FFV is about 0.04–0.05 in isotropic amorphous polyesters and decreases as orientation brings the polymer closer to the equilibrium (zero solubility) condition. Jump length (the dynamic free-volume component) is calculated from the activation energy of diffusivity and is found to be about 14 Å. This is consistent with the dimension of a simple cubic lattice based on the free volume hole density reported in the literature. The corresponding hole size obtained from the measured excess-hole free volume is 2.6 to 3.1 Å, which correlates well with the hole radius obtained from PALS. It follows from the model that only a small fraction of the free volume holes are occupied at any instant. However, very rapid dif-

fusion kinetics means that the small number of permeant molecules share all the excess-free volume holes and justifies the macroscopic concept of sorbed gas density. The time scale of the actual jump is extremely short, and the oxygen molecule spends most of the time in the hole in accordance with the general understanding of activated gas diffusion.

This research was generously supported by the National Science Foundation (DMR 9975774 and DMR 9986467) and KoSa. Support from Modern Controls, Inc. for development of a facility for gas-transport studies at Case Western Reserve University is gratefully acknowledged.

REFERENCES AND NOTES

- Slee, J. A.; Orchard, G. A. J.; Bower, D. I.; Ward, I. M. *J Polym Sci Part B: Polym Phys* 1989, 27, 71–83.
- Orchard, G. A. J.; Spiby, P.; Ward, I. M. *J Polym Sci Part B: Polym Phys* 1990, 28, 603–621.
- Holden, P. S.; Orchard, G. A. J.; Ward, I. M. *J Polym Sci B: Polym Phys* 1985, 23, 2295–2306.
- Theodorou, D. N. In *Diffusion in Polymers*; Neogi, P., Ed.; New York: Marcel Dekker, 1996; Chap. 2, pp 67–142.
- Polyakova, A.; Liu, R. Y. F.; Schiraldi, D. A.; Hiltner, A.; Baer, E. *J Polym Sci Part B: Polym Phys* 2001, 39, 1889–1899.
- Polyakova, A.; Connor, D. M.; Collard, D. M.; Schiraldi, D. A.; Hiltner, A.; Baer, E. *J Polym Sci Part B: Polym Phys* 2001, 39, 1900–1910.
- Liu, R. Y. F.; Schiraldi, D. A.; Hiltner, A.; Baer, E. *J Polym Sci Part B: Polym Phys* 2002, 40, 862–877.
- Sekelik, D. J.; Stepanov, S. V.; Nazarenko, S.; Schiraldi, D.; Hiltner, A.; Baer, E. *J Polym Sci Part B: Polym Phys* 1999, 37, 847–857.
- Polyakova, A.; Stepanov, E. V.; Sekelik, D.; Schiraldi, D. A.; Hiltner, A.; Baer, E. *J Polym Sci Part B: Polym Phys* 2001, 39, 1911–1919.
- Lin, J.; Shenogin, S.; Nazarenko, S. *Polymer* 2002, 43, 4733–4743.
- Hu, Y. S.; Liu, R. Y. F.; Zhang, L. Q.; Rogunova, M.; Schiraldi, D. A.; Nazarenko, S.; Hiltner, A.; Baer, E. *Macromolecules* 2002, 35, 7326–7337.
- Park, J. Y.; Paul, D. R. *J Membr Sci* 1997, 125, 23–39.
- Thran, A.; Kroll, G.; Faupel, F. *J Polym Sci Part B: Polym Phys* 1999, 37, 3344–3358.
- Tonelli, A. E. *Polymer* 2002, 43, 637–642.
- Parravicini, L.; Leone, B.; Auriemma, F.; Guerra, G.; Petraccone, V.; Dino, G. D.; Bianchi, R.; Vosa, R. *J Appl Polym Sci* 1994, 52, 875–885.
- Busico, V.; Corradini, P.; Riva, F. *Makromol Chem Rapid Commun* 1980, 1, 423–426.

17. Kluin, J. E.; Yu, Z.; Vleeshouwers, S.; McGervey, J. D.; Jamieson, A. M.; Simha, R.; Sommer, K. *Macromolecules* 1993, 26, 1853–1861.
18. Michaels, A. S.; Vieth, W. R.; Barrie, J. A. *J Appl Phys* 1963, 34, 1–12.
19. Michaels, A. S.; Vieth, W. R.; Barrie, J. A. *J Appl Phys* 1963, 34, 13–20.
20. Van Krevelen, D. W. In *Properties of Polymers*, 3rd ed. Boca Raton, FL: CRC, 1990; Chap. 4, pp 71–108.
21. Weiss, G. H.; Bendler, J. T.; Shlesinger, M. F. *Macromolecules*, 1992, 25, 990–992.
22. Vrentas, J. S. Duda, J. L. *J Appl Polym Sci* 1978, 22, 2325–2339.
23. Liu, R. Y. F.; Hu, Y. S. Hibbs, M. R.; Collard, D. M.; Schiraldi, D. A.; Hiltner, A.; Baer, E. *J Polym Sci Part B: Polym Phys* 2003, 41, 289–307.
24. Ma, H.; Hibbs, M.; Collard, D. M.; Kumar, S.; Schiraldi, D. A. *Macromolecules* 2002, 35, 5123–5130.
25. Williams, M.; Landel, R. F.; Ferry, J. D. *J Am Chem Soc* 1955, 77, 3701–3707.
26. Simha, R.; Boyer, R. F. *J Chem Phys* 1962, 37, 1003–1007.
27. Petropoulos, J. H. In *Polymeric Gas Separation Membranes*; Paul, D. R.; Yampol'ski, Y. P., Eds.; Boca Raton, FL: CRC, 1994; Chap. 2, pp 17–82.
28. Meares, P. *J Am Chem Soc* 1954, 76, 3415–3422.
29. Duda, J. L.; Zielinski, J. M. In *Diffusion in Polymers*; Neogi, P., Ed.; New York: Marcel Dekker, 1996; Chap. 3, pp 143–172.
30. Takeuchi, H. *J Chem Phys* 1990, 93, 2062–2067.
31. Greenfield, M. L.; Theodorou, D. N. *Macromolecules* 1998, 31, 7068–7090.
32. Simha, R.; Somcynsky, T. *Macromolecules* 1969, 2, 342–350.
33. Rane, S.; Gujrati, P. D. *Phys Rev E* 2001, 64, 011801.
34. Srithawatpong, R.; Peng, Z. L.; Olson, B. G.; Jamieson, A. M.; Simha, R.; McGervey, J. D.; Maier, T. R.; Halasa, A. F.; Ishida, H. *J Polym Sci Part B: Polym Phys* 1999, 37, 2754–2770.
35. Dlubek, G.; Bondarenko, V.; Pionteck, J.; Supej, M.; Wutzler, A.; Krause-Rehberg, R. *Polymer* 2003, 44, 1921–1926.
36. Bamford, D.; Dlubek, G.; Reiche, A.; Alam, M. A.; Meyer, W.; Galvosas, P.; Rittig, F. *J Chem Phys* 2001, 115, 7260–7270.
37. Hong, X.; Jean, Y. C.; Yang, H.; Jordan, S. S.; Koros, W. J. *Macromolecules* 1996, 29, 7859–7864.
38. Schrader, D. M.; Jean, Y. C., Eds. In *Positron and Positronium Chemistry*; Elsevier: Amsterdam, 1988; Chap. 1, pp 1–26.
39. Liu, R. Y. F.; Hiltner, A.; Baer, E. Unpublished results.